

# Multimode Interference: Identifying Channels and Ridges in Quantum Probability Distributions

Ross C. O'Connell\*  
*Department of Physics*  
*University of Michigan*  
*Ann Arbor, MI 48104*

Will Loinaz†  
*Department of Physics*  
*Amherst College*  
*Amherst, MA 01002*

The multimode interference technique is a simple way to study the interference patterns found in many quantum probability distributions. We demonstrate that this analysis not only explains the existence of so-called “quantum carpets,” but can explain the spatial distribution of channels and ridges in the carpets. With an understanding of the factors that govern these channels and ridges we have a limited ability to produce a particular pattern of channels and ridges by carefully choosing the weighting coefficients  $c_n$ . We also use these results to demonstrate why fractional revivals of initial wavepackets are themselves composed of many smaller packets.

## I. INTRODUCTION

The existence of multiple time scales in many simple, one-dimensional quantum systems is both an important characteristic that distinguishes them from their classical counterparts and the source of many interesting phenomena in the time-evolution of those systems. Let us begin with a wavefunction of the form

$$\Psi(x, t) = \sum_{n=1}^{\infty} c_n \psi_n(x) e^{-iE_n t}, \quad (1)$$

where  $\psi_n$  is the  $n$ th eigenfunction,  $E_n$  the energy of the  $n$ th eigenfunction, and the  $c_n$  are weighting coefficients. The most straightforward way to identify the time scales is to treat  $E_n$  as a function of  $n$  and perform a Taylor expansion of the energy around some quantum number  $\bar{n}$ , the number around which the weighting coefficients are centered,

$$E_n \approx E_{\bar{n}} + E'_{\bar{n}}(n - \bar{n}) + \frac{1}{2!} E''_{\bar{n}}(n - \bar{n})^2 + \dots \quad (2)$$

We identify the time scales as

$$\frac{2\pi}{T_j} = \frac{E_{\bar{n}}^{(j)}}{\hbar j!}. \quad (3)$$

The  $T_j$  almost always obey the hierarchy  $T_1 \ll T_2 \ll T_3 \dots$ , as is demonstrated in Appendix A.  $T_1$  corresponds to the classical period of a particle of energy  $E_{\bar{n}}$ , so we call it  $T_{cl}$ . At times near  $T_2$  the contribution from the  $E''_{\bar{n}}(n - \bar{n})$  terms to the phase of each eigenfunction will be negligible. When the aforementioned hierarchy holds, the contribution from the  $T_j$  terms for  $j > 3$  will also be negligible and the classical behavior governed by  $T_{cl}$  will dominate, approximately reproducing the  $t \approx 0$  behavior of the particle. The return of the wavefunction to its  $t \approx 0$  value is called a quantum revival, and we call  $T_2$  the revival time,  $T_R$ . The literature on the subject of revivals is well-developed, including several general articles [1, 7, 27], treatments of fractional revivals [2, 3, 16, 21, 26], and articles on possible applications of this phenomenon [4, 8, 19]. Revivals are also analogous to the Talbot effect in classical electrodynamics, as is discussed in [5, 6, 11, 20].

We wish to explain the behavior of the wavefunction at times comparable to, but not equal to,  $T_R$ . At these times, in problems with anharmonic spectrum and for wavefunctions  $\Psi(x, t)$  in which the distribution of  $c_n$  has central value

---

\*Electronic address: rcoconne@umich.edu

†Electronic address: waloinaz@amherst.edu

$\bar{n}$  and characteristic width  $\Delta n$  which obey the hierarchy  $1 \ll \Delta n \ll \bar{n}$  (a semiclassical case), the spacetime diagram of the probability distribution exhibits a complex pattern of channels and ridges – what has come to be called a quantum carpet. The problem has been approached with several techniques [12, 14, 15, 22, 23], and finds application in study of Bose-Einstein condensates [9, 28, 29]. In this paper, we develop the technique of multimode interference [17, 18]. In section II we briefly review the multimode interference technique and introduce characteristic velocities. In section III we obtain, in the context of the WKB approximation, the characteristic velocities of channels and ridges in the spacetime diagram of the probability distribution, and in section IV we examine the way in which the degeneracy of these velocities shapes the quantum carpet. These ideas are illustrated with the example of the infinite square well potential in section V and are used to elucidate the structure of fractional revivals in section VI. Section VII offers a summary of lessons learned.

## II. MULTIMODE INTERFERENCE AND CHARACTERISTIC VELOCITIES

A multimode term is a straightforward adaptation of a density matrix element,

$$\mu_{nm}(x, t) = d_{nm} \psi_n(x) \psi_m^*(x) e^{-it(E_n - E_m)}, \quad (4)$$

$$d_{nm} = c_n c_m^* = d_{mn}^*, \quad (5)$$

which allows us to write a probability density as

$$\|\Psi(x, t)\|^2 = \sum_{n, m=1}^{\infty} \mu_{nm}(x, t). \quad (6)$$

While the multimode terms lack some of the convenient properties of the density matrix they can simplify the study of some dynamic phenomena, since they allow us to write the probability density as a simple sum. Of course, in order to do much with them we will have to make an assumption about the eigenfunctions.

We will use the WKB approximation [13] to obtain a usable form of the eigenfunctions,  $\psi_n$ . While this limits the range of applicability of our findings, quantum probability distributions only acquire the features that earn the name “quantum carpet” in the semiclassical case [30]. The approximate eigenfunctions are

$$\psi_n(x) \approx \frac{C_n^{(-)}}{\sqrt{p_n(x)}} \exp\left(i \int^x p_n(x') dx'\right) + \frac{C_n^{(+)}}{\sqrt{p_n(x)}} \exp\left(-i \int^x p_n(x') dx'\right), \quad (7)$$

where the  $C_n^{(\pm)}$  are complex constants of integration, and

$$p_n(x) = \sqrt{E_n - V(x)}. \quad (8)$$

The approximate multimode terms  $\mu_{nm}$  will be weighted sums of four intermode terms,

$$\mu_{nm} \approx d_{nm} \left( \iota_{nm}^{(++)} + \iota_{nm}^{(+-)} + \iota_{nm}^{(-+)} + \iota_{nm}^{(--) } \right), \quad (9)$$

where

$$\iota_{nm}^{(\pm_1 \pm_2)}(x, t) = d_{nm} \frac{C_n^{(\pm_1)} C_m^{(\pm_2)}}{\sqrt{p_n(x) p_m(x)}} \exp -i \left( \int^x (\pm_1 p_n(x') \pm_2 p_m(x')) dx' + (E_n - E_m) t \right). \quad (10)$$

We are interested in features of the probability density that are time-dependent and typically much more “narrow” than the potential, so we focus our attention on the phase factor instead of the leading factors of  $p_n^{-1/2}$ . We can characterize the curves of constant phase by differentiating the argument of the exponential and looking for its roots,

$$\frac{d}{dt} \left( \int^{x(t)} (\pm_1 p_n(x') \pm_2 p_m(x')) dx' + (E_n - E_m) t \right) = 0, \quad (11)$$

$$\frac{dx}{dt} = - \frac{E_n - E_m}{\pm_1 p_n(x) \pm_2 p_m(x)}, \quad (12)$$

$$v_{nm}^{(\pm_1 \pm_2)} = \frac{\Delta \omega}{\Delta k} = - \frac{E_n - E_m}{\pm_1 \sqrt{E_n - V(x)} \pm_2 \sqrt{E_m - V(x)}}, \quad (13)$$

we find that each pair of quantum numbers,  $(n, m)$ , gives rise to *four* velocities  $v_{nm}^{(\pm_1 \pm_2)}$ . We can pick any one of these velocities, integrate it from an arbitrary  $x_0$ , and the resulting trajectory is a line of constant phase. Channels and ridges in the probability distribution follow these lines, as we will demonstrate in section IV.

### III. CHARACTERIZATION OF THE VELOCITIES

We have written eq. 13 as  $\Delta\omega/\Delta k$  anticipating that we will label some of the velocities as “group velocities.” Defining  $\omega_n = E_n$  and  $k_n(x) = p_n(x)$ , we can write

$$\omega_n(k_n, x) = k_n^2 - V(x). \quad (14)$$

We now make the additional assumption that the weighting coefficients are well-centered on some number  $\bar{n}$  with some spread  $\Delta n$ , and that these satisfy the hierarchy  $1 \ll \Delta n \ll \bar{n}$ . This allows us to define a group velocity for our packet,

$$v_{gr} = \left. \frac{d\omega_n}{dk_n} \right|_{n=\bar{n}} = 2k_{\bar{n}}, \quad (15)$$

which is the classical velocity of a particle in the potential  $V$  with energy  $E_{\bar{n}}$ .

Writing  $E_n = E_{\bar{n}} + e_n$  and  $E_m = E_{\bar{n}} + e_m$ , where  $e_n, e_m \ll E_{\bar{n}} - V(x)$ , we can simplify our expression for the velocities in eq. 13,

$$\begin{aligned} v_{nm}^{(\pm_1\pm_2)} &= -\frac{(E_{\bar{n}} + e_n) - (E_{\bar{n}} + e_m)}{\pm_1\sqrt{E_{\bar{n}} + e_n - V(x)} \pm_2\sqrt{E_{\bar{n}} + e_m - V(x)}} \\ &\approx -\frac{e_n - e_m}{\sqrt{E_{\bar{n}} - V(x)} \left( \pm_1 \left( 1 + \frac{e_n}{2(E_{\bar{n}} - V(x))} \right) \pm_2 \left( 1 + \frac{e_m}{2(E_{\bar{n}} - V(x))} \right) \right)} \\ &\approx -2\sqrt{E_{\bar{n}} - V(x)} \frac{e_n - e_m}{2(E_{\bar{n}} - V(x)) (\pm_1 1 \pm_2 1) + (\pm_1 e_n \pm_2 e_m)} \\ &\approx \begin{cases} \pm 2\sqrt{E_{\bar{n}} - V(x)} = \pm 2k_{\bar{n}}(x), & (+1-2, -1+2) \\ \pm \frac{e_n - e_m}{2\sqrt{E_{\bar{n}} - V(x)}} \approx \pm \frac{\omega_n - \omega_m}{2k_{\bar{n}}(x)}, & (+1+2, -1-2). \end{cases} \end{aligned} \quad (16)$$

As long as both  $e_n, e_m \ll E_{\bar{n}} - V(x)$ , as is required in the semiclassical approximation, then half of the velocities contributed by a particular  $(n, m)$  are comparable to the group velocity,  $v_{gr}$ , and half are smaller. It is important to note (in preparation for the next section) that eq. 16 is approximate – it is *not* the case that half of the velocity terms are exactly degenerate.

### IV. GROUPS OF VELOCITIES AND DEGENERACY

The result in eq. 16 demonstrates that in any problem there exists a range of velocities. Though that result was approximate, we will now show that some intermode terms have *exactly* the same maximum velocities, and that because of this we can treat those intermode terms as essentially moving together. This is a sort of degeneracy – the sort of degeneracy that produces quantum carpets.

If we examine the velocities (eq. 13) at a point where  $V(x) = 0$ , we find that

$$v_{nm}^{(\pm_1\pm_2)} = -\frac{E_n - E_m}{\pm_1\sqrt{E_n} \pm_2\sqrt{E_m}}. \quad (17)$$

We can factor the numerator,

$$v_{nm}^{(\pm_1\pm_2)} = -\frac{(\sqrt{E_n} + \sqrt{E_m})(\sqrt{E_n} - \sqrt{E_m})}{\pm_1\sqrt{E_n} \pm_2\sqrt{E_m}}, \quad (18)$$

and arrive at an important condition,

$$v_{nm}^{(\pm_1\pm_2)} = \mp_1\sqrt{E_n} \pm_2\sqrt{E_m}. \quad (19)$$

Terms that have the same  $v_{nm}^{(\pm_1\pm_2)}$  at  $V(x) = 0$  change phase with the same period – these are our degenerate terms.

We define a group of velocities as

$$\beta_v(x, t) = \sum_{|v_{nm}^{(\pm_1\pm_2)}|=v} \iota_{nm}^{(\pm_1\pm_2)}(x, t). \quad (20)$$

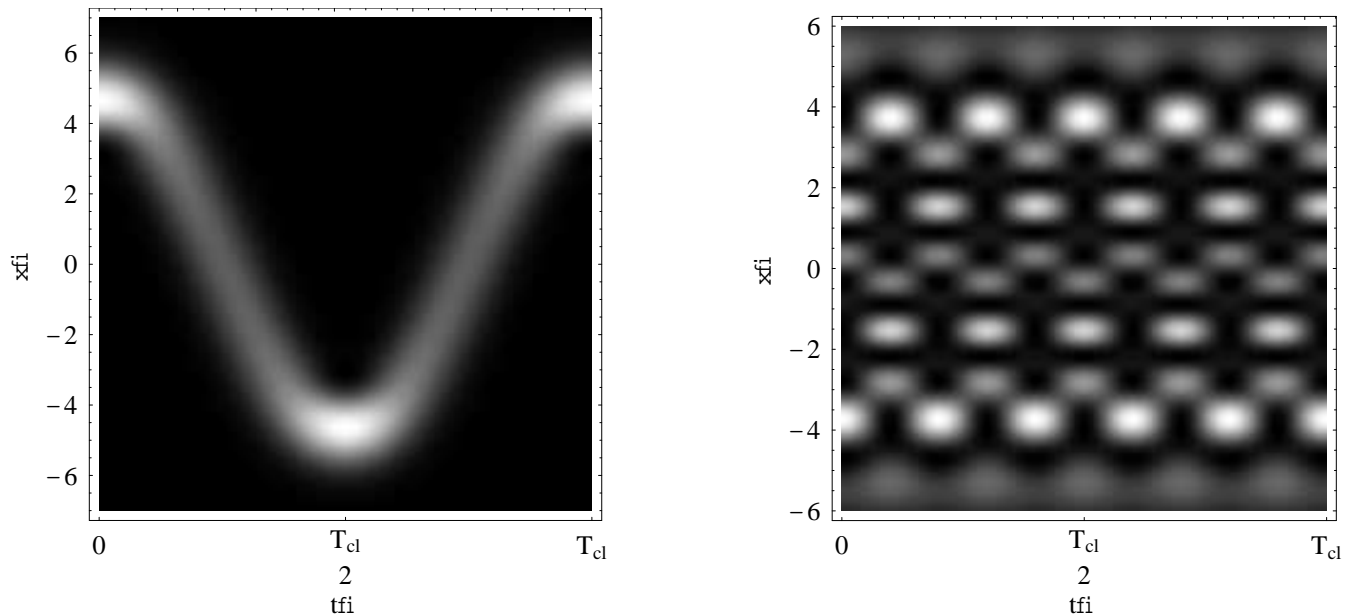


Figure 1: Two plots of the simple harmonic oscillator. On the left, the distribution of coefficients is Gaussian, with  $\bar{n} = 6$  and  $\sigma_n = 2$ , while the plot on the right is an even weighting of the perfect squares between 1 and 81.

Because the first sign in the definition of the velocities (eq. 19) is flipped relative to the signs in the definition of an intermode term (eq. 10), each  $\beta_v$  will look roughly like a weighted sum of harmonic functions. If there are many terms in the sum, they may interfere to produce a peak or a valley. As the wavefunction evolves in time, these peaks and valleys will trace out the canals and ridges that form the quantum carpet.

This immediately demonstrates the role of quadratic spectra in producing quantum carpets. If the spectrum depends on the quantum number  $n$  squared, then there will be many degenerate velocities, while if the spectrum is linear in the quantum number, only traces which involve two perfect squares may be degenerate. This suggests that if we begin with a system like the simple harmonic oscillator, with a spectrum linear in the quantum number, and set to zero all weighting coefficients that are not perfect squares (selecting only states 1,4,9,16, etc.), we can produce a carpet because we have effectively “quadrated” the spectrum [31]. For an example of this, see Figure 1.

## V. THE INFINITE SQUARE WELL

We now turn our attention to a particular example in order to illustrate the utility of these results. We write explicitly all of the relevant physical constants, so as to facilitate comparison with classical results. For a particle of mass  $M$  in a well of width  $L$  we have the wavefunction,

$$\Psi(x, t) = \sqrt{\frac{2}{L}} \sum_{n=1}^{\infty} c_n \frac{i}{2} \left( \exp\left(i\frac{n\pi}{L}x\right) - \exp\left(-i\frac{n\pi}{L}x\right) \right) \exp\left(-i\frac{\hbar\pi^2 n^2}{2ML^2}t\right). \quad (21)$$

We can immediately identify the velocities in question as

$$v_{nm}^{\pm_1 \pm_2} = \frac{\hbar\pi}{2ML} (\mp_1 n \pm_2 m) = v_0 (\mp_1 n \pm_2 m). \quad (22)$$

We can also find that the wavenumbers  $k_{nm}$  will be

$$k_{nm}^{\pm_1 \pm_2} = \frac{\pi}{L} (\pm_1 n \pm_2 m), \quad (23)$$

so that in any particular velocity bundle there will be a variety of wavenumbers. We provide an example of the interference that this produces in figure 2.

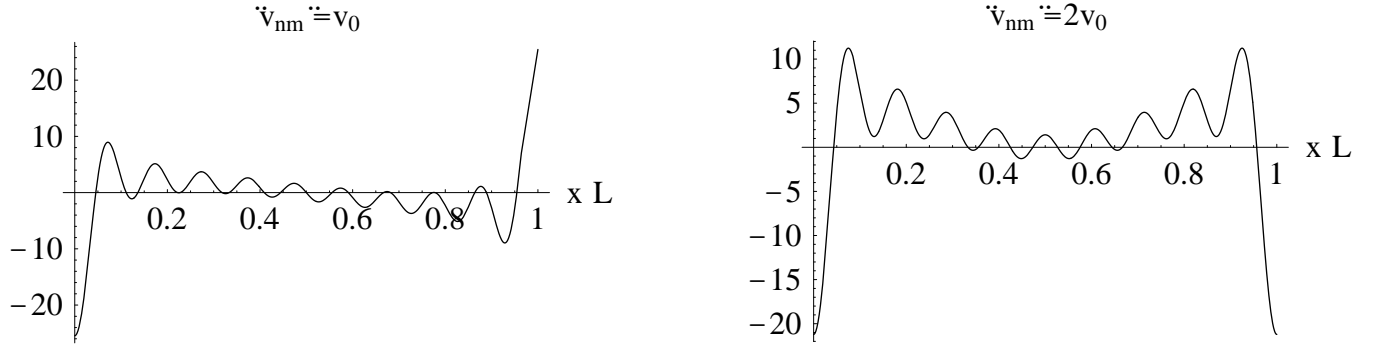


Figure 2: The  $|v_{nm}| = v_0$  (left) and  $|v_{nm}| = 2v_0$  (right) velocity bundles for a uniform distribution of weighting coefficients between  $n = 1$  and  $n = 10$  in the infinite square well.

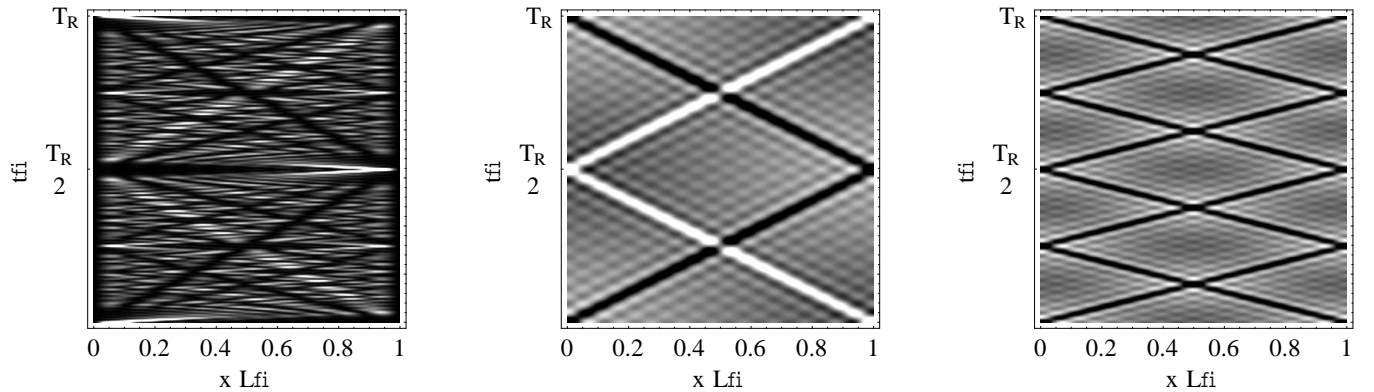


Figure 3: At left, the full carpet, coefficients evenly weighted between  $n = 1$  and  $n = 10$ . In the middle, the eighteen intermode terms that compose  $\beta_{v_0}$ . Note that they do, indeed, have a period  $T = T_R$ . At right the 34 intermode terms that compose  $\beta_{2v_0}$ . Note that they have a period  $T = T_R/2$ .

The most degenerate velocity will typically be  $v_0$ , and in time  $T_R = 2L/v_0$  a trajectory with this velocity will cover a distance of  $2L$ , so the most prominent traces should have the same period as the revival time. Better still, we can ask what velocity we need in order to have a period equal to the classical period,  $T_{cl}$ . The condition is

$$\begin{aligned} v_{nm}T_{cl} &= v_{nm}\frac{L}{\bar{n}v_0} = 2L \\ v_{nm} &= 2\bar{n}v_0, \end{aligned} \quad (24)$$

which should be satisfied by very few  $(n, m)$  pairs. An example of how well our separation of the wavefunction works is shown in Figure 3.

In the case of the square well we can find a closed form for  $\beta_v(x, 0)$ . From the definition and the form of  $v_{nm}^{(\pm_1\pm_2)}$  it can be shown that

$$\begin{aligned} \beta_v(x, t) &= \left( -\sum_{n=1}^{\infty} \frac{c_n c_{n+v}^*}{4} \left( \iota_{n(n+v)}^{(++)}(x, t) + \iota_{n(n+v)}^{(--)}(x, t) \right) - \sum_{m=1}^{\infty} \frac{c_{m+v} c_m^*}{4} \left( \iota_{(m+v)m}^{(++)}(x, t) + \iota_{(m+v)m}^{(--)}(x, t) \right) \right. \\ &\quad \left. + \sum_{n=1}^{v-1} \frac{c_n c_{v-n}^*}{4} \left( \iota_{n(v-n)}^{(+-)}(x, t) + \iota_{n(v-n)}^{(-+)}(x, t) \right) \right) \end{aligned}$$

and recalling that the  $\iota_{nm}^{(\pm_1\pm_2)}$  are just exponentials, we can write  $\beta_v(x, 0)$  as

$$\beta_v(x, t) = \frac{2}{L} \sum_{n=1}^{\infty} \text{Re} \{ c_n c_{n+v}^* \} \cos \left( (2n+v) \frac{\pi x}{L} \right) + \frac{1}{L} \cos \left( v \frac{\pi x}{L} \right) \sum_{n=1}^{v-1} c_n c_{v-n}^*. \quad (25)$$

The first term contributes peaks and valleys, while the second sets a threshold height above which those peaks and valleys must rise in order to be visible. The first term suggests that we can, by choosing appropriate  $c_n$ , control the distribution of peaks and valleys, though we cannot generate an arbitrary function [32].

## VI. MULTIMODE TRACES AND QUANTUM REVIVALS

In problems where the weighting coefficients  $c_n$  are well-localized around some central quantum number  $\bar{n}$ , so that the spectrum can be well approximated by

$$E_n \approx E_{\bar{n}} + E'_{\bar{n}}(n - \bar{n}) + \frac{1}{2}E''_{\bar{n}}(n - \bar{n}) = E_{\bar{n}} + \frac{2\pi}{T_{cl}}k + \frac{2\pi}{T_R}k^2, \quad (26)$$

we can make an interesting approximation to the wavefunction at rational fractions of  $T_R$ . We do not present the details of the derivation here (see [3] or [25]), but quote the result that

$$\Psi\left(x, t \approx \frac{p}{q}T_R\right) \approx \sum_{s=0}^{l-1} a_s \Psi_{cl}\left(x, t + \frac{s}{l}T_{cl}\right), \quad (27)$$

where  $l = q/2$  when  $q$  contains more than one power of two,  $l = q$  otherwise, the  $a_s$  are complex weighting coefficients (for their values, see [3] or [25]), and we have defined

$$\Psi_{cl}(x, t) = \sum_{k=-\infty}^{\infty} c_{k+\bar{n}} \psi_{k+\bar{n}}(x) \exp\left(-2\pi i k \frac{t}{T_{cl}}\right). \quad (28)$$

This approximation states that the wavefunction can be written as the sum of slices of a ‘‘classitized’’ wavefunction,  $\Psi_{cl}$ . It suggests that at rational fractions of  $T_R$  (particularly fractions with low  $q$ ), a wavefunction that began as a well-localized packet will consist of several packets. We will now demonstrate that if  $\Psi(x, t = 0)$  is well-localized, then  $\Psi_{cl}$  will remain well-localized for all  $t$ .

Observe from the derivation of Equation 13 that the  $E_n - E_m$  term comes from the time-evolution exponential and the square root terms come from the WKB approximation. If we want to find a similar formula for  $\Psi_{cl}$ , we need only replace the  $E_n - E_m$  in the numerator with  $(2\pi/T_1)(n - m)$ . Considering a point where  $V(x) = 0$ , we find the following velocity degeneracy condition:

$$v_{nm} = \pm_1 \frac{2\pi}{T_{cl}} \frac{n - m}{\sqrt{E_n} \pm_2 \sqrt{E_m}}. \quad (29)$$

Unlike Equation 19, we have no hope of factoring this in general. We can, however, see what happens in a few obvious cases. If

$$E_n = \alpha^2 n, \quad (30)$$

then we quickly find

$$v_{nm} = \pm_1 \frac{2\pi}{T_{cl}\alpha} \frac{n - m}{\sqrt{n} \pm_2 \sqrt{m}}, \quad (31)$$

a degeneracy condition identical to the one we would have found for the harmonic oscillator in the previous section. If, however, we try a spectrum  $E_n = \alpha^2 n^2$ , we find something far more interesting,

$$v_{nm} = \pm_1 \frac{2\pi}{T_{cl}\alpha} \frac{n - m}{n \pm_2 m} = \begin{cases} \pm_1 \frac{2\pi}{T_{cl}\alpha}, & (-2), \\ \pm_1 \frac{2\pi}{T_{cl}\alpha} \frac{n-m}{n+m}, & (+2). \end{cases} \quad (32)$$

*Half* of all of the traces are degenerate! Looking at the other half, we want to find two pairs of numbers,  $(n, m)$  and  $(p, q)$  that will be degenerate. The conditions are

$$\frac{n - m}{n + m} = \frac{p - q}{p + q}, \quad n + m \neq 0, \quad p + q \neq 0, \quad n \neq p, \quad m \neq q, \quad (33)$$

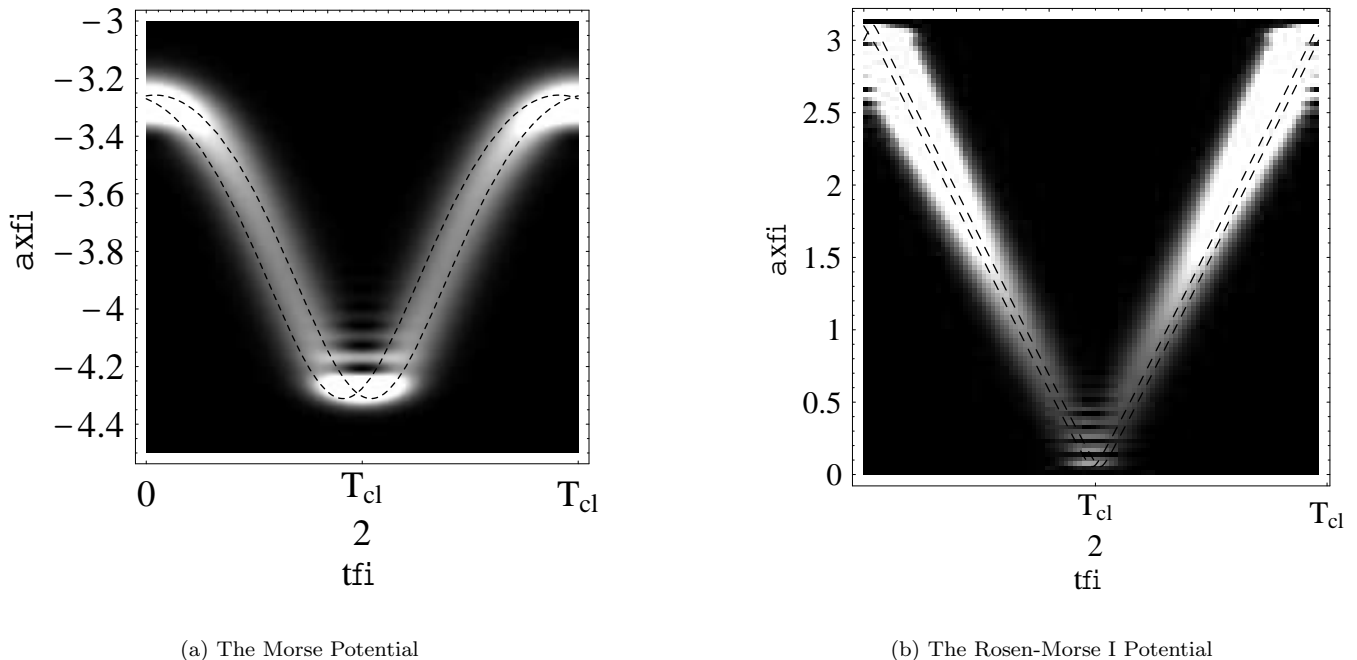


Figure 4: Plots of  $\Psi_{cl}$  in two potentials, one with a quadratic spectrum and one with a non-quadratic spectrum. On the left is the Morse Potential, with  $E_n = A^2 - (A - \alpha n)^2$ , and on the right the Rosen-Morse I potential, with  $E_n = -A^2 + (A + \alpha n)^2 - (B/(A + \alpha n))^2 + (B/A)^2$ . In both cases  $A$ ,  $B$ , and  $\alpha$  are independent constants. The black lines overlaying the maxima are classical paths for those potentials with  $E = E_{\bar{n}}$ . These are exactly solvable potentials taken from [10].

which then reduce to

$$\begin{aligned}
 (p+q)(n-m) &= (n+m)(p-q), \\
 qn - mp &= -qn + mp, \\
 \frac{n}{m} &= \frac{p}{q}.
 \end{aligned} \tag{34}$$

While this is not a difficult equation to satisfy with all of the integers at our disposal, it is difficult to satisfy when our weighting coefficients are all within some  $\Delta n \ll \bar{n}$  of  $\bar{n} \gg 1$ . The solutions that will lie closest to  $(n, m)$  are  $(p, q) = 1/2(n, m)$  and  $(p, q) = 2(n, m)$ . If  $n$  and  $m$  are in the vicinity of  $\bar{n}$ , as they must be in the semiclassical case, that puts  $p$  and  $q$  near either  $\bar{n}/2$  or  $2\bar{n}$ , both of which would typically be “out of range” of  $\Delta n$ . For the case of a quadratic spectrum, then, we find that half of the velocities are degenerate, and that the other half tend to be non-degenerate. This nicely corresponds with our suspicion that  $\Psi_{cl}$  wavepackets evolve along classical paths.

The unfortunate aspect of this result for  $\Psi_{cl}$  is that it is so heavily dependent on the quadratic character of the spectrum. This behavior seems to occur in potentials with non-quadratic spectra as well, as demonstrated in Figure 4. However, in the semiclassical limit (that is, for very large  $\bar{n}$ ), their spectra can appear to be no more than quadratic [24]. This leaves low- $\bar{n}$  cases to consider, and completing our understanding of  $\Psi_{cl}$  is a possible subject for future work.

## VII. SUMMARY

We have seen how an analysis of the intermode terms in the probability density of a semiclassical wavefunction can give us insight into the degeneracy conditions which must be met in order to produce a carpet, and into the carpet itself. When those degeneracy conditions are met, we can examine the initial form of certain bundles of velocities and from that find the channels and ridges of the quantum carpet. For a problem with a spectrum linear in the quantum number it was almost impossible to generate a carpet, though a perverse choice of weighting coefficients could effectively quadratize the spectrum. Similar reasoning suggested why  $\Psi_{cl}$  should so often resemble a classically oscillating packet, and thus why fractional revivals of a wavepacket should themselves resemble the initial packet.

**Appendix A: DEMONSTRATION THAT  $T_1 \ll T_2 \ll T_3 \dots$**

We begin by assuming that our spectrum can be written as a polynomial in  $n$ ,

$$E_n = \sum_{m=1}^M a_m n^m. \quad (\text{A1})$$

In this case, the  $j$ th derivative of  $E_n$  is

$$E_n^{(j)} = \sum_{m=j}^M a_m n^m \left( \frac{m!}{(m-j)!n^j} \right), \quad (\text{A2})$$

and if  $n > m - j$  the  $j$ th derivative will reduce the contribution from the  $n$ th term. So long as  $\bar{n} \gg M$ , it will be true that  $E_n^{(1)} \gg E_n^{(2)} \gg E_n^{(3)} \dots$ , since  $\frac{m!}{n!} < \frac{M!}{n!} \ll 1$ . Consequently,  $T_1 \ll T_2 \ll T_3 \dots$  holds. Our result is not significantly changed by allowing negative powers of  $n$ . Consider

$$E_n = \sum_{m=1}^M a_m n^{-m}. \quad (\text{A3})$$

Its derivatives are

$$E_n^{(j)} = \sum_{m=1}^M a_m n^{-m} (-1)^j \left( \frac{(m+j-1)!}{(m-1)!n^j} \right), \quad (\text{A4})$$

so we still get that  $T_1 \ll T_2 \ll T_3 \dots$  so long as  $\bar{n} \gg M$ . Transcendental spectra still present a problem, though we note that the spectrum of *any* one-dimensional potential cannot increase faster than  $n^2$  for large  $n$ , roughly because the walls of the potential cannot be “harder” than the infinite square well [24].

- [1] Aronstein, D. L. (2000). Analytical investigation of revival phenomena in the finite square-well potential. *Physical Review A*, 62:022102.
- [2] Aronstein, D. L. and Stroud, C. R. J. (1997). Fractional wave-function revivals in the infinite square well. *Physical Review A*, 55(6):4526–4537.
- [3] Averbukh, I. S. and Perelman, N. (1989). Fractional revivals: Universality in the long-term evolution of quantum wave packets beyond the correspondence principle dynamics. *Physics Letters A*, 139(9):449–453.
- [4] Averbukh, I. S. and Perelman, N. (1991). The dynamics of wave packets of highly-excited states of atoms and molecules. *Sov. Phys. Usp.*, 34(7):572–591.
- [5] Berry, M. V. and Bodenschatz, E. (1999). Caustics, multiply reconstructed by talbot interference. *Journal of Modern Optics*, 46(2):349–365.
- [6] Berry, M. V. and Klein, S. (1996). Integer, fractional, and fractal talbot effects. *Journal of Modern Optics*, 43(10):2139–2164.
- [7] Bluhm, R., Kostelecky, V. A., and Porter, J. A. (1996). The evolution and revival structure of quantum wave packets. *American Journal of Physics*, 64:944.
- [8] Chen, X. and Yeazell, J. A. (1998). Analytical wave-packet design scheme: Control of dynamics and creation of exotic wave packets. *Physical Review A*, 57(4):R2274–R2277.
- [9] Choi, S., Burnett, K., Friesch, O. M., Kneer, B., and Schleich, W. (2001). Spatiotemporal interferometry for trapped atomic bose-einstein condensates. *Physical Review A*, 63:065601. cond-mat/0011468.
- [10] Cooper, F., Khare, A., and Sukhatme, U. (2001). *Supersymmetry in Quantum Mechanics*. World Scientific Publishing Co.
- [11] Dubra, A. and Ferrari, J. A. (1999). Diffracted field by an arbitrary aperture. *American Journal of Physics*, 67(1):87–92.
- [12] Friesch, O., Marzoli, I., and Schleich, W. P. (2000). Quantum carpets woven by wigner functions. *New Journal of Physics*, 2(4):4.1–4.11.
- [13] Griffiths, D. J. (1995). *Introduction to quantum mechanics*. Prentice Hall, Englewood Cliffs, N.J.
- [14] Grossmann, F., Rost, J.-M., and Schleich, W. P. (1997). Spacetime structures in simple quantum systems. *Journal of Physics A*, 30:L277–L283.
- [15] Hall, M. J., Reineker, M. S., and Schleich, W. P. (1999). Unravelling quantum carpets: A travelling wave approach. *Journal of Physics A: Mathematics and General*, 32:8275–8291. quant-ph/9906107 v2.
- [16] Jie, Q.-L., Wang, S.-J., and Wei, L.-F. (1998). Partial revivals of wave packets: An action-angle phase-space description. *Physical Review A*, 57(5):3262–3267.



- [17] Kaplan, A., Marzoli, I., Lamb, W. J., and Schleich, W. (2000). Multimode interference: Highly regular pattern formation in quantum wave-packet evolution. *Physical Review A*, 61:032101.
- [18] Kaplan, A., Stifter, P., van Leeuwen, W., Lamb, W. J., and Schleich, W. P. (1998). Intermode traces-fundamental interference phenomenon in quantum and wave physics. *Physica Scripta*, T76:93–97.
- [19] Knospe, O. and Schmidt, R. (1996). Revivals of wave packets: General theory and application of rydberg clusters. *Physical Review A*, 54(2):1154–1160.
- [20] Lock, J. A. and Andrews, J. H. (1992). Optical caustics in natural phenomena. *American Journal of Physics*, 60(5):397–407.
- [21] Loinaz, W. and Newman, T. (1999). Quantum revivals and carpets in some exactly solvable systems. *Journal of Physics A: Mathematics and General*, 32:8889–8895. quant-ph/9902039.
- [22] Marzoli, I., Bialynicki-Biruli, I., Friesch, O., Kaplan, A., and Schleich, W. (1998a). The particle in the box: Intermode traces in the propagator. quant-ph/9804015.
- [23] Marzoli, I., Saif, F., Bialynicki-Birula, I., Friesch, O., Kaplan, A., and Schleich, W. (1998b). Quantum carpets made simple. *Acta Physica Slovaca*, 48(3):323–333. quant-ph/9806033.
- [24] Nieto, M. M. and Simmons, L. J. (1979). Limiting spectra from confining potentials. *American Journal of Physics*, 47(7):634–635.
- [25] O’Connell, R. (2002). A foray into quantum dynamics. Amherst College Honors Thesis, quant-ph/0212092.
- [26] Razi Naqvi, K., Waldenstrom, S., and Haji Hassan, T. (2001). Fractional revival of wave packets in an infinite square well: a fourier perspective. *European Journal of Physics*, 22:395–402.
- [27] Rozmej, P. and Arvieu, R. (1998). Clones and other interference effects in the evolution of angular-momentum coherent states. *Physical Review A*, 58(6):4314–4329. quant-ph/9801018.
- [28] Ruostekoski, J., Kneer, B., Schleich, W. P., and Rempe, G. (2001). Inteferece of a bose-einstein condensate in a hard-wall trap: From the nonlinear talbot effect to the formation of vorticity. *Physical Review A*, 63:043613. cond-mat/9908095.
- [29] Wright, E. M., Wong, T., Collett, M. J., Tan, S. M., and Walls, D. F. (1997). Collapses and revivals in the interference between two bose-einstein condensates formed in small atomic samples. *Physical Review A*, 56(1):591–602. cond-mat/9611211.
- [30] The term “semiclassical” is a bit ambiguous. Although a distribution of weighting coefficients  $c_n$  that satisfies  $1 \ll \Delta n \ll \bar{n}$  seems to be most important in producing semiclassical behavior we are here willing to relax this to the WKB assumption that the potential changes much more slowly than the relevant eigenfunctions oscillate. Note that  $\Delta n \gg 1$  implies  $\Delta p \gg 1$ , which in turn suggests (via the uncertainty principle) that  $\Delta x \ll 1$ , and thus that the WKB approximation is appropriate.
- [31] “Effectively quadratize the spectrum” is shorthand for choosing weighting coefficients such that only terms that have quantum numbers that are perfect squares are contained in the wavefunction. When we do this, we could rewrite the spectrum, eigenfunctions, etc., as if they were governed by a new variable,  $m^2 = n$ , as if they had quadratic spectra. Of course, we’re not changing the spectrum itself, we’re changing the wavefunction.
- [32] Note here that a choice of  $1, 1, -1, -1, 1, 1, -1, -1$  for the  $c_n$ , with  $c_n = 0$  for  $n > 8$ , yields a  $\beta_{v_0}(x, 0)$  with a peak and a valley at the center of the well, and  $\beta_{v_0} = 0$  at the walls of the well. This contradicts the assertion about the distribution of peaks and valleys contained in [17].